ACS APPLIED MATERIALS & INTERFACES

Research Article

www.acsami.org

Low-Cost Counter Electrodes From CoPt Alloys For Efficient Dye-Sensitized Solar Cells

Benlin He, Xin Meng, and Qunwei Tang*

Institute of Materials Science and Engineering, Ocean University of China, Qingdao 266100, P.R. China

ABSTRACT: Dye-sensitized solar cell (DSSC) is a promising solution to global energy and environmental problems because of its merits on clean, low cost, high efficiency, good durability, and easy fabrication. However, the commercial application of DSSCs has been hindered by the high expenses of counter electrodes (CEs) and limited power conversion efficiency. With an aim of significantly enhancing the power conversion efficiency, here we pioneerly synthesize CoPt alloys using an electrochemically codeposition technique which are employed as CEs for DSSCs. Owing to the rapid charge transfer, electrical conduction, and electrocatalysis, power conversion efficiencies of CoPt-based DSSCs have been markedly elevated in comparison with the DSSC using Pt CE. The DSSC employing $CoPt_{0.02}$ alloy CE gives an impressive power conversion efficiency of 10.23%. The high conversion efficiency, low cost in combination with simple preparation, and scalability demonstrates the potential use of CoPt alloys in robust DSSCs.

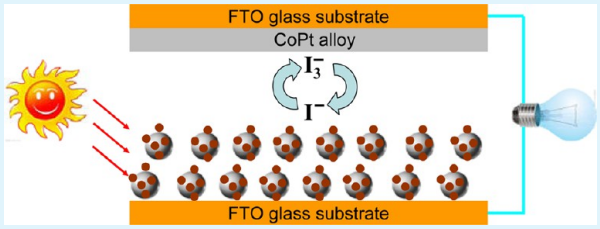

KEYWORDS: *Counter electrodes, Low-Pt composites, CoPt alloys, Dye-sensitized solar cells*

INTRODUCTION

Since the first prototype from O'Regan and Grätzel, dye-sensitized solar cells (DSSCs) have attracted growing interests because they are a promising solution to global energy and environmental problems.[1] However, DSSC is still an emerging concept in the new solar cell technologies relying on thin films. For commercial application, key challenges include the demonstration of high power conversion efficiency and low cost of counter electrode (CE).[2−4] As one of the heavy expenses in DSSCs, Pt CE is a burden for large-scale fabrication because it is a relatively precious metal.[5] Therefore, it is a prerequisite to develop facile, cheap, as well as efficient CE materials for large-scale DSSC assembly. Considering that the mission of a CE is the reduction of redox species used as a mediator in regenerating the sensitizer after electron injection in a liquid-state/quasi-solid-state DSSC, or collection of the holes from the hole-conducting material in a solid-state DSSC, conducting polymers and carbon materials as well as their composites have been employed to meet all of these requirements because of their low electrical resistance, reversible redox, facile synthesis, good environmental stability, and low cost. The unsatisfactory conversion efficiency (~7.0%) gets them in a dilemma.[6−10] Alloy CEs are new class of materials that combine high electrical conductivity, superior electrocatalytic activity, and low cost. Wang et al. synthesized $Co_{0.85}Se$ and $Ni_{0.85}Se$ non-Pt alloy CEs by a low-temperature hydrothermal approach. The proposed metal selenides exhibited much higher electrocatalytic activity than Pt for reduction of triiodide, and generated a promising power conversion efficiency of 9.40%.[11] More recently, an alloy CE from $CuInGaSe_2$ alloy has been prepared by a magnetron sputtering technology, giving a conversion efficiency of 7.13% in its DSSC device.[12] Moreover, Au−Ag binary alloy can also be employed as counter electrode material in DSSC, demonstrating a conversion efficiency of 7.85%.[13] However, the unfavorable power conversion efficiency is still a tremendous obstacle for alloy CEs in robust DSSCs.

To significantly enhance the power conversion efficiency of alloy-based DSSCs, herein, we develop an alternative strategy for the synthesis of a new type of low-Pt binary alloy by an electrochemical codeposition method. Considering the potentially electrochemical behaviors of transition elements, Co is employed to combine with Pt. Regarding the efficient electrocatalyst, resultant CoPt alloy CEs demonstrate intrinsic electrocatalytic activity for the reduction of triiodide ions, rapid charge-transfer ability, and low expenses. The DSSCs composed of $CoPt_{0.02}$ alloy CEs shows a conversion efficiency as high as 10.23%, which is much higher than 6.52% from expensive Pt CE-based DSSC. The high-performance of $CoPt_{0.02}$ alloy CE is originated from the synergetic effect between Co and Pt.[14−16]

EXPERIMENTAL SECTION

Preparation of CoPt Alloy CEs. The feasibility of this strategy was confirmed by following experimental procedures: Cleaned FTO glass substrate (sheet resistance 12 Ω^{-1}, purchased from Hartford Glass Co., USA) was immersed in a mixing aqueous solution consisting of H_2PtC1_6 and $Co(NO_3)_2$ aqueous solutions in 20 mmol L^{-1} of HCl at a Pt/Co (mol/mol) of 1:100, 1:50, 1:25, 1:10, 1:5. The CoPt alloy CEs were electrochemically codeposited by a potentiostatic method at a potential of −0.5 V and a deposition time of 250 s.

Received: December 11, 2013
Accepted: March 10, 2014
Published: March 10, 2014

dx.doi.org/10.1021/am405706q | *ACS Appl. Mater. Interfaces* 2014, 6, 4812−4818

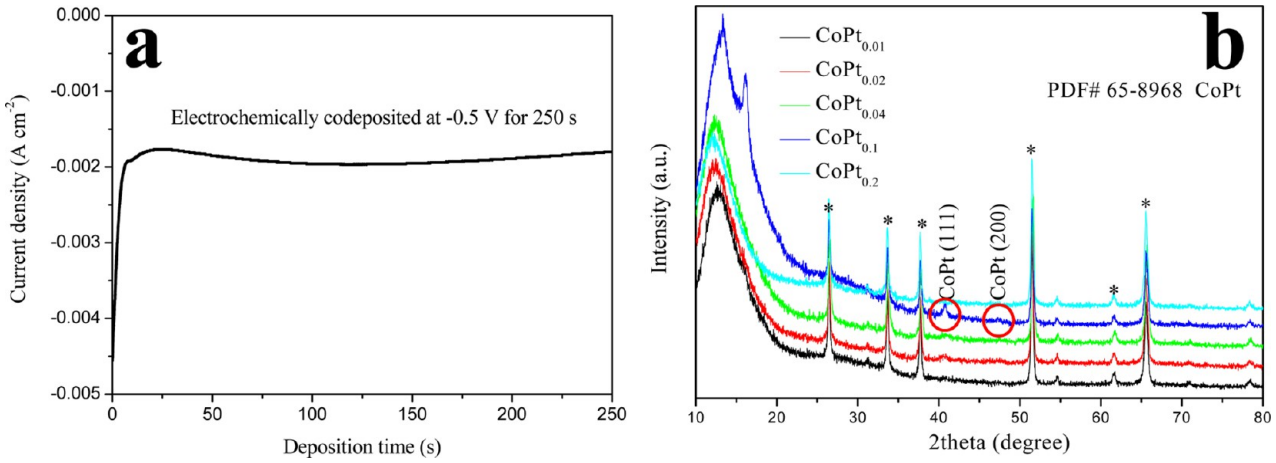

Figure 1. (a) Electrochemically codeposition curves of $CoPt_{0.02}$ alloy on FTO glass substrate. (b) XRD patterns of CoPt alloy CEs.

Assembly of DSSCs. A layer of TiO_2 nanocrystal anode film with a thickness of 10 μm was prepared by a sol-hydrothermal method and a layer of TiO_2 nanocrystal anode film with a thickness of 10 μm and an active area of 0.25 cm^2 was prepared by coating TiO_2 colloid onto conducting glass using a doctor blade technique, followed by sintering in air at 450 °C for 30 min. Resultant anodes were further sensitized by immersing into a 0.50 mM ethanol solution of N719 dye ([cis-di(thiocyanato)-N,N′-bis(2,2′-bipyridyl-4-carboxylic acid)-4-tetrabutylammonium carboxylate]). The DSSC was fabricated by sandwiching redox electrolyte between dye-sensitized TiO_2 anode and FTO supported CoPt alloy CEs. A redox electrolyte consisted of 100 mM tetraethylammonium iodide, 100 mM tetramethylammonium iodide, 100 mM tetrabutylammonium iodide, 100 mM NaI, 100 mM KI, 100 mM LiI, 50 mM I_2, and 500 mM 4-tert-butyl-pyridine in 50 mL of acetonitrile.

Electrochemical Characterizations. The electrochemical performances were recorded on a conventional CHI660E setup comprising an Ag/AgCl reference electrode, a CE of platinum sheet, and a working electrode of FTO glass supported CoPt alloy. The cyclic voltammetry (CV) curves were recorded from −0.6 to +1.4 V and back to−-0.6 V. Before the measurement, the supporting electrolyte consisting of 50 mM M LiI, 10 mM I_2, and 500 mM $LiClO_4$ in acetonitrile was degassed using nitrogen for 10 min. Electrochemical impedance spectroscopy (EIS) measurements were also carried out on the CHI660E Electrochemical Workstation in a frequency range of 0.01 Hz to ~1 × 10^6 kHz and an ac amplitude of 5 mV at room temperature. The resultant impedance spectra were analyzed using the Z-view software. Tafel polarization curves were recorded on the same Workstation by assembling symmetric cell consisting of FTO/CoPt alloy|redox electrolyte|FTO/CoPt alloy.

Photovoltaic Measurements. The photocurrent−-voltage (J−V) curves of the assembled DSSCs were recorded on an Electrochemical Workstation (CHI600E) under irradiation of a simulated solar light from a 100 W xenon−mercury arc lamp (CHF-XM-500W, Beijing Trusttech Co., Ltd) in an ambient atmosphere. The incident light intensity was calibrated using a FZ-A type radiometer from Beijing Normal University Photoelectric Instrument Factory to control it at 100 mW cm^{-2} (AM 1.5). Each DSSC device was measured five times to eliminate experimental error and a compromise J−V curve was employed.

Other Characterizations. The morphologies of the $CoPt_{0.02}$ alloy CE were observed with a scanning electron microscope (SEM, S4800). The XRD data were collected in a scan mode with a scanning speed of 10° min^{-1} in the 2θ range between 10 and 80°. Incident photo-to-current conversion efficiency (IPCE) curves were obtained at the short-circuit condition on an IPCE measurement systems (MS260). The light source in this case was a solar simulator (PEC-L11, AM1.5G, Peccell Technologies, Inc.); the light was focused through a monochromator onto the photovoltaic cell. The monochromator was moved in steps from 400 to 700 nm to generate the IPCE. To obtain the IPCE spectra, we sensitized the anodes by N719 dye. The compositions of the alloy CEs were detected by inductively coupled plasma-atomic emission spectra (ICP-AES). Prior to ICP measurements, the alloy CEs were immersed in concentration nitric acid to dissolve the FTO glass substrate thoroughly.

RESULTS AND DISCUSSION

Structure and Morphology Characterizations. The electrochemical codeposition curve of $CoPt_{0.02}$ alloy on FTO glass substrate is shown in Figure 1a. Rapid increase in current density indicates the durative codeposition of alloy material with relatively high electrical conduction. The CoPt alloys are subjected to X-ray diffraction (XRD) measurements. As shown in Figure 1b, XRD results indicate that the as-prepared samples consist of CoPt (fm-3m, PDF# 65-8968) and bared FTO layer (PDF# 46-1088). The compositions of the alloys on FTO glass substrate were determined by ICP-AES equipment. The results display that the atomic ratios of $CoPt_{0.01}$, $CoPt_{0.02}$, $CoPt_{0.04}$, $CoPt_{0.1}$, and $CoPt_{0.2}$ are 1.000:0.008, 1.000:0.016, 1.000:0.042, 1.000:0.087, and 1.000:0.183, respectively. The measured atomic ratios are close to the stoichiometry of $CoPt_{0.01}$, $CoPt_{0.02}$, $CoPt_{0.04}$, $CoPt_{0.1}$, and $CoPt_{0.2}$; therefore, the chemical formulae of the alloy CEs can be expressed according to their stoichiometric ratios. Scanning electron microscopy (SEM) in Figure 2a suggests a higher surface coverage and loading of $CoPt_{0.02}$ on FTO substrate in comparison with surface morpholigies of CoPt0.01 (Figure 2c) and CoPt0.2 (Figure 2d) alloy CEs. Deep examination in Figure 2b gives homogeneously spherical aggregations at ~80 nm. The relatively loose structure between aggregations provide channels for triiodide ions across the alloy layer.[17,18] From energy-dispersive X-ray spectrum, as shown in Figure 2e, Pt and Co elements as well as the elements from FTO substrate are detected, indicating that Pt and Co have been successfully codeposited on FTO glass substrate.

Photovoltaic Performance of DSSCs. Figure 3a shows J−V curves of the DSSCs using CoPt alloy and Pt (300−400 μm in thickness, purchased from Dalian HepatChroma SolarTech Co., Ltd) as CEs. The detailed photovoltaic parameters from the J−V curves are summarized in Table 1. The DSSC with $CoPt_{0.02}$ CE yields a remarkable η of 10.23%, J_{sc} of 18.53 mA cm^{-2}, V_{oc} of 0.735 V, and FF of 0.751, whereas the DSSC with pure Pt CE gives a η of 6.52%, J_{sc} of 13.93 mA cm^{-2}, V_{oc} of 0.714 V, and FF of 0.66. Evidently, J_{sc} increases in an order of Pt < $CoPt_{0.2}$ < $CoPt_{0.01}$ < $CoPt_{0.1}$ < $CoPt_{0.04}$ < $CoPt_{0.02}$, and the

dx.doi.org/10.1021/am405706q | ACS Appl. Mater. Interfaces 2014, 6, 4812−4818

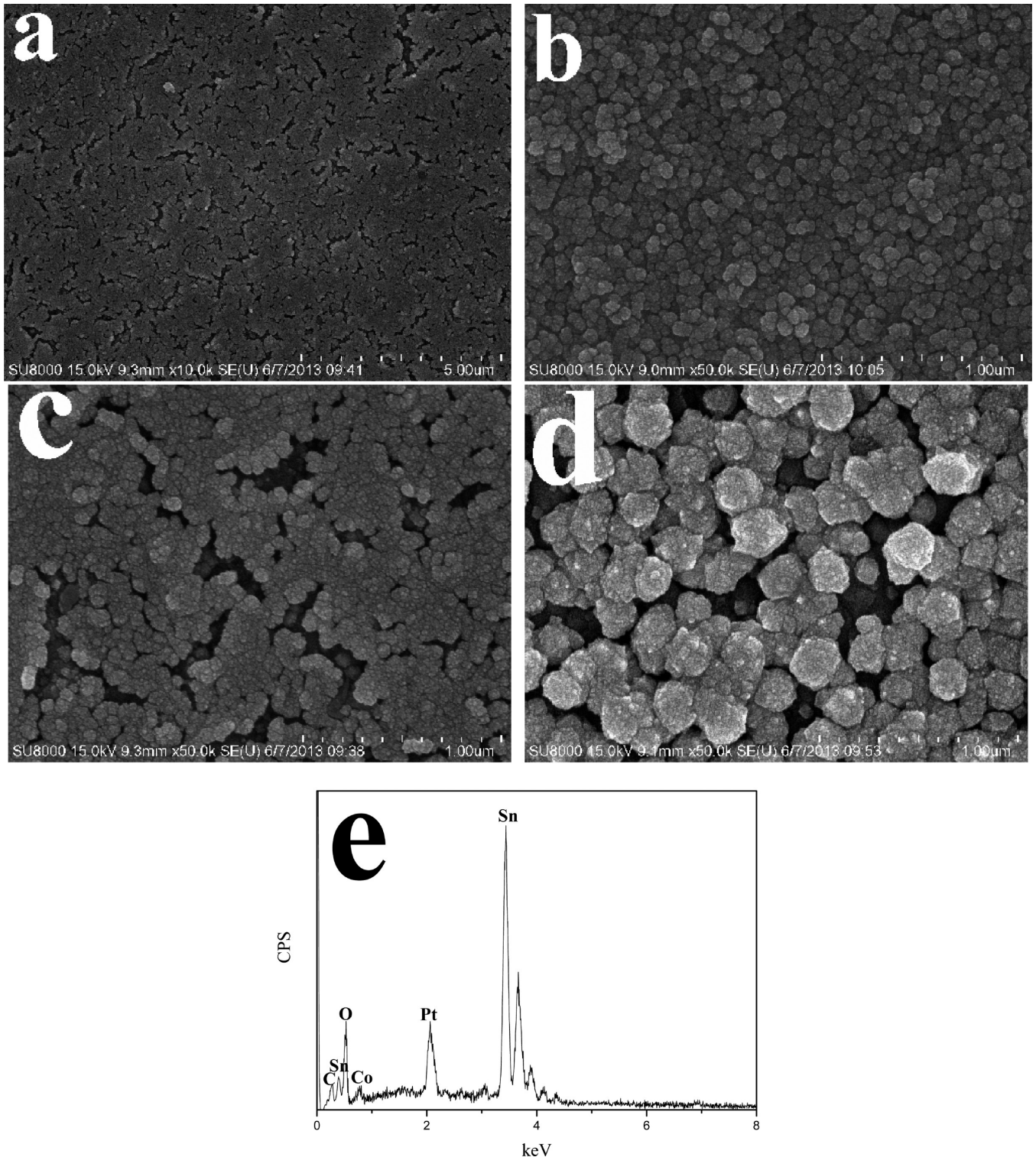

Figure 2. (a, b) SEM images of $CoPt_{0.02}$ alloy on FTO glass at different magnifications. SEM photographs of (c) $CoPt_{0.01}$ and (d) $CoPt_{0.2}$ alloy CEs. (e) Energy-dispersive X-ray spectrum of $CoPt_{0.02}$ alloy CE.

η increases in the same order. The recorded efficiencies from CoPt alloy CEs are impressive for low-Pt electrocatalysts in DSSCs. To the best of our knowledge, this is the highest η for I^-/I_3^- redox couple based DSSCs with low-Pt or non-Pt CEs under AM1.5G simulated solar light (100 mW cm^{-2}).[11−13,19] As a reference, a Co-only CE is also been prepared by the electrochemical deposition method and assembled into a DSSC device. A power conversion efficiency of 1.84% is obtained because of the poor electrocatalytic activity toward triiodide ions and poor charge-transfer ability. In the case of employing similar TiO_2 anode, the significant enhancement in photovoltaic performances is a comprehensive reflection of electrocatalytic activity toward triiodides and charge-transfer ability of CoPt alloy CEs. The relatively high *FF* is of highly dependent on the sheet resistance (R_s) of CEs. From EIS plots of DSSCs in Figure 3b and Figure 3c, one can find that the $CoPt_{0.02}$ alloy

dx.doi.org/10.1021/am405706q | *ACS Appl. Mater. Interfaces* 2014, 6, 4812−4818

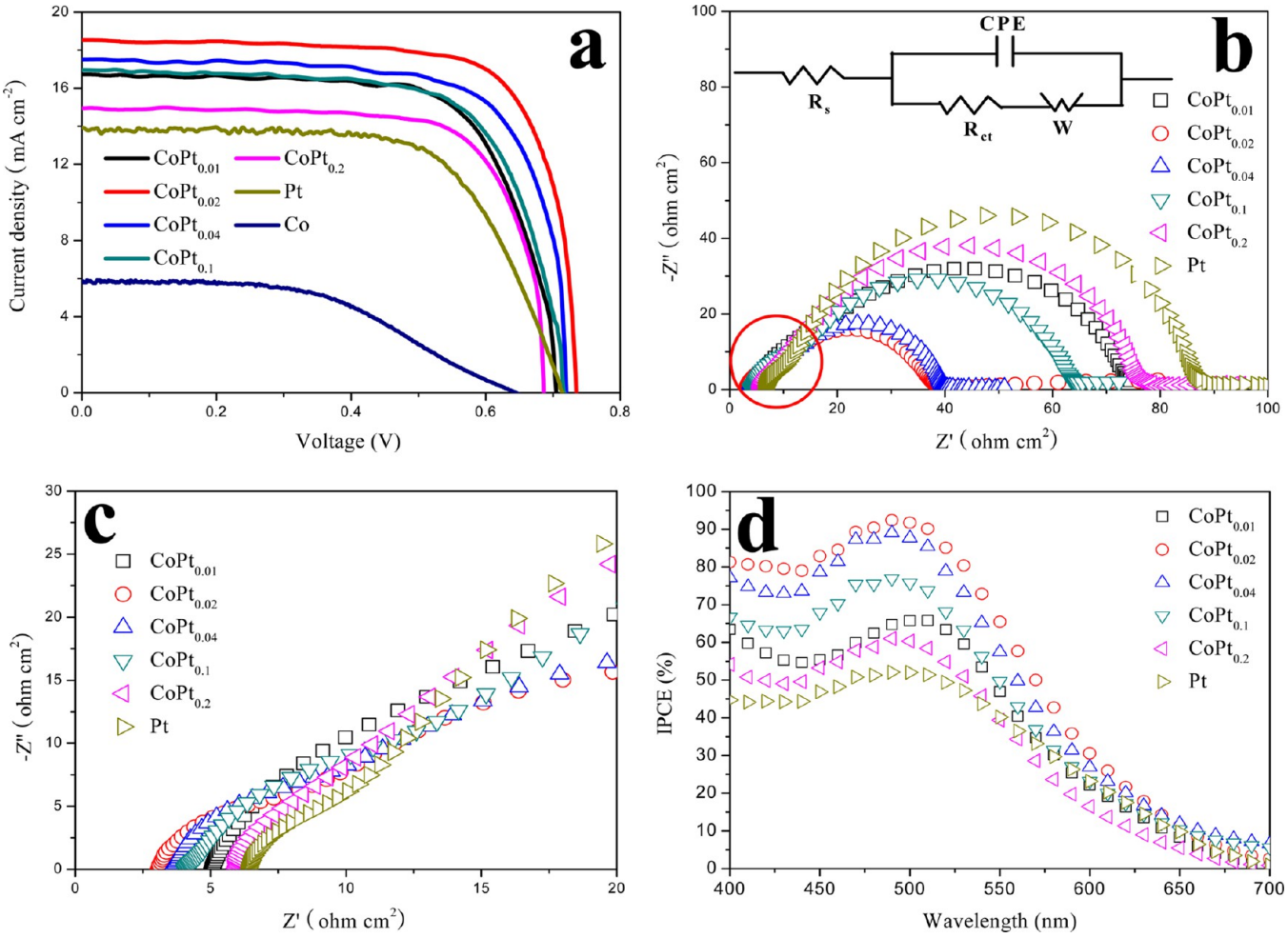

Figure 3. (a) Characteristic *J*–*V* curves, (b, c) EIS spectra, and (d) IPCE plots of DSSCs from varied CEs.

Table 1. Photovoltaic Parameters of DSSCs with Varied CEs and the Simulated Data from EIS Spectra Using Symmetric Cells[a]

CEs	η (%)	V_{oc} (V)	*FF*	J_{sc} (mA cm^{-2})	R_{ct} (Ω cm^2)
CoPt$_{0.01}$	8.29	0.705	0.70	16.75	9.50
CoPt$_{0.02}$	10.23	0.735	0.75	18.53	0.68
CoPt$_{0.04}$	9.18	0.721	0.73	17.46	1.57
CoPt$_{0.1}$	8.43	0.715	0.70	16.95	3.29
CoPt$_{0.2}$	7.59	0.688	0.74	14.95	5.17
Pt	6.52	0.714	0.66	13.93	13.00
Co	1.84	0.643	0.50	5.78	17.35

[a] V_{oc}, open-circuit voltage; J_{sc}, short-circuit current densit; *FF*, fill factor; η, power conversion efficiency; R_{ct}, charge-transfer resistance.

CE has the lowest R_s (the intercept on the real axis), whereas Pt CE exhibits the largest R_s value. Therefore, The DSSC from CoPt$_{0.02}$ alloy CE has a higher *FF*. The maximum incident monochromatic photon-to-electron conversion efficiency (IPCE) is 92.4% at CoPt$_{0.02}$ alloy CE, as shown in Figure 3d, but it is only 52.1% for Pt-only CE. Deep examination demonstrates that the IPCE is a comprehensive reflection of light-harvesting efficiency, charge-collection efficiency, and charge-injection efficiency.[20] The elevation of IPCE value reveals that the formation of CoPt alloy CEs has significantly enhanced the generation of electrons into photocurrent, in which CoPt$_{0.02}$ alloy CE exhibits the highest photon-to-electron conversion efficiency.

Electrochemical Behaviors of CoPt Alloy CEs. The effect of CE on DSSC performance is mainly derived from its electrocatalytic activity toward reduction of triiodide to iodide and electron conduction.[5,11] In the cyclic voltammograms (CVs), as shown in Figure 4, the peak positions of the CoPt

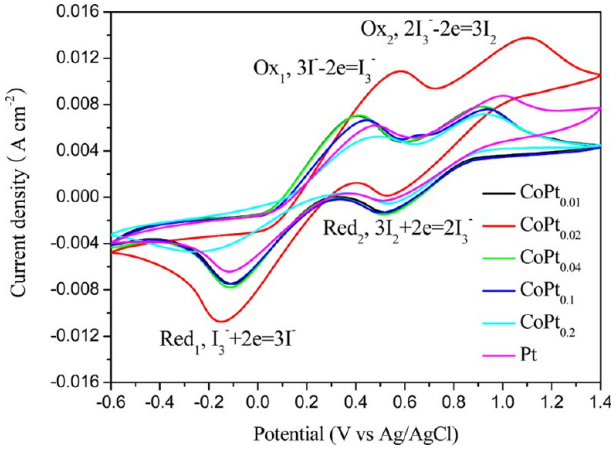

Figure 4. CV curves of CoPt alloy and Pt CEs for I^-/I_3^- redox species recorded at a scan rate of 50 mV s^{-1}.

dx.doi.org/10.1021/am405706q | ACS Appl. Mater. Interfaces 2014, 6, 4812–4818

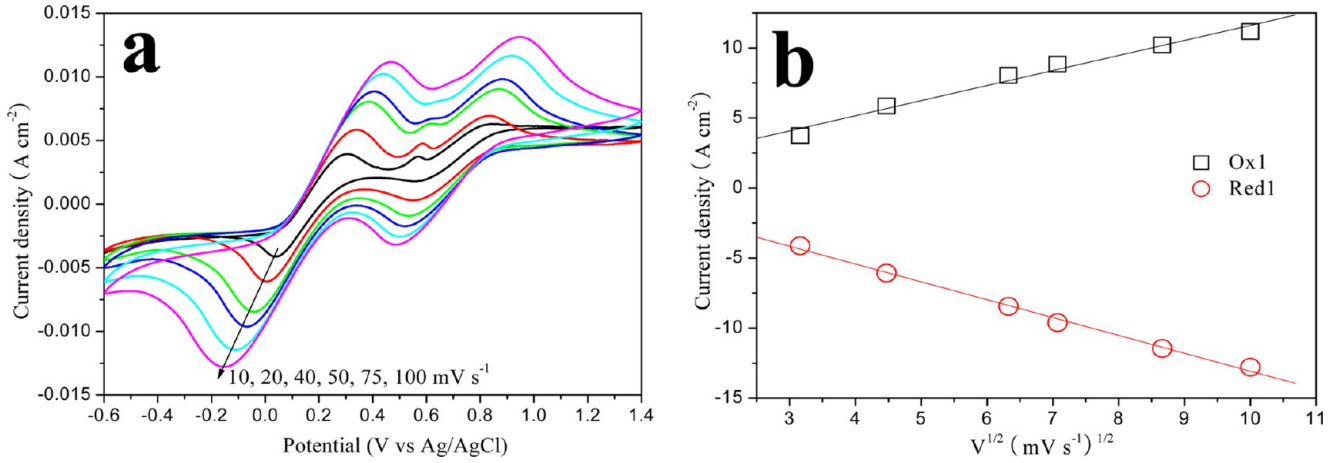

Figure 5. (a) CV curves of $CoPt_{0.02}$ alloy CE for I^-/I_3^- redox species at different scan rates (from inner to outer: 10, 20, 40, 50, 75, and 100 mV s^{-1}), and (b) relationship between peak current density and square root of scan rates.

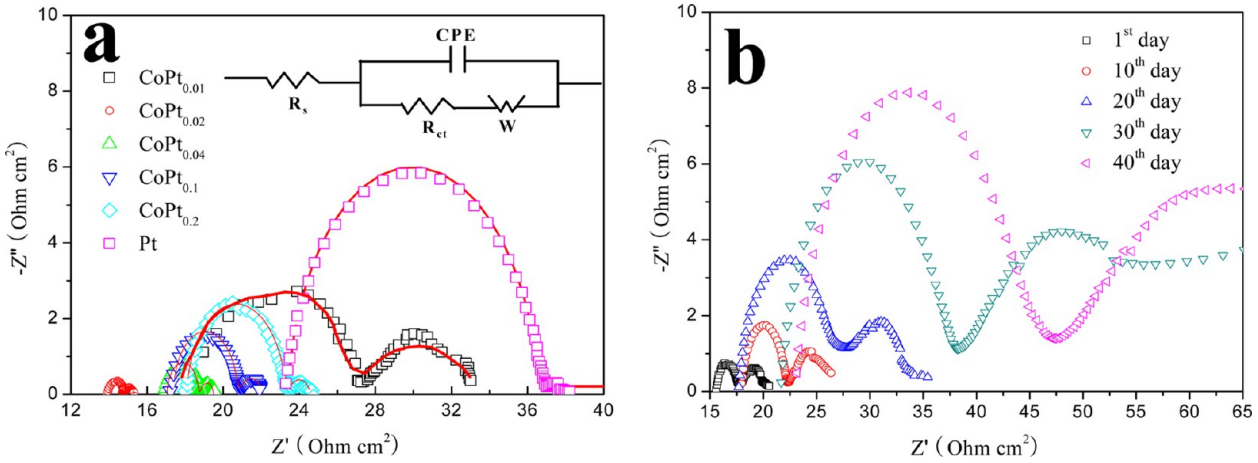

Figure 6. (a) Nyquist plots for symmetric cells fabricated double CoPt alloy or double Pt CEs. The lines express fitting results for corresponding EIS data, and the inset gives the equivalent circuit. (b) EIS spectra of the DSSCs from $CoPt_{0.02}$ alloy CE subjected to aging for 40 days at room temperature and open circuit.

alloys are very similar to that of Pt electrode, showing that CoPt alloys have a similar electrocatalytic function to the Pt electrode. Furthermore, CoPt alloy CEs have higher current densities, suggesting higher electrocatalytic activity.[21,22] Considering that the task of CE is the reduction of redox species used as a mediator in regenerating the sensitizer after electron injection in a liquid-state DSSC. The electroreduction reaction of $I_3^- + 2e \rightarrow 3\ I^-$ can be employed to elevate the electrocatalytic activity of CoPt alloy CEs. A catalytic activity enhancement of 1.5-fold is achieved for $CoPt_{0.02}$ CE in comparison to a benchmark Pt CE. Only the alloy CE with a Pt:Co ratio of 0.2:1 is displayed for lower catalytic activity than Pt CE. The employment of alloy CE in DSSCs is a pioneering work, however, that is relatively popular in fuel cells.[23−27] Xu et al. demonstrated that alloying of Co can effectively tune the electron structure of Pt because the alloying of Co and Pt can lower the d-band center of Pt.[27] It is expected that the molar amount of Co at 0.02 mol % can bring most favorable electronic perturbation for Pt electron structure. Similar promotion effect has also been found in NiPt alloys.[27,28] Notably, the ratio of $J_{ox1}/|J_{red1}|$ is a parameter to elevate the reversibility of the redox reaction toward I^-/I_3^-.[29] The obtained value from $CoPt_{0.02}$ alloy CE (0.966) is closer to 1.0 than $CoPt_{0.01}$ (0.914), $CoPt_{0.04}$ (0.940), $CoPt_{0.1}$ (1.062), $CoPt_{0.2}$ (1.118), and Pt (0.947), indicating a more reversible redox reaction for $I_3^- \leftrightarrow I^-$. The rapid recovery of iodides to their ground state facilitates the participation in subsequent circles and improves the long-term stability. Randles-Sevcik theory is employed to elucidate the diffusion of iodide in CE,[30] giving diffusion coefficients ($cm^{-2}\ s^{-1}$) for $CoPt_{0.01}$, $CoPt_{0.02}$, $CoPt_{0.04}$, $CoPt_{0.1}$, $CoPt_{0.2}$, and Pt CEs of 1.94×10^{-5}, 3.18×10^{-5}, 2.10×10^{-5}, 1.98×10^{-5}, 7.78×10^{-6}, and 1.44×10^{-5}, respectively. Results indicate that the CoPt alloys can accelerate the diffusion kinetics of iodide species within CEs.

From the stacking CV curves of $CoPt_{0.02}$ alloy CE at different scan rates, one can find an outward extension of all the peaks (Figure 5a). By plotting peak current density corresponding to $I_3^- \leftrightarrow I^-$ versus square root of scan rate, as shown in Figure 5b, linear relationships are observed. This result indicates the redox reaction is a diffusion-controlled mechanism on $CoPt_{0.02}$ alloy CE.[31] This may be the result from transport of iodide species on CE surfaces.

Nyquist plots in Figure 6a illustrate impedence characteristics of CoPt alloy and Pt CEs, in which two semicircles are observed. A Randles-type circuit is obtained by fitting EIS spectra using a Z-view software, and there is a good agreement between recorded and fitted curves. The R_{ct} values of all CoPt alloy CE are all smaller than that of Pt electrode, indicating a

dx.doi.org/10.1021/am405706q | ACS Appl. Mater. Interfaces 2014, 6, 4812−4818

promoting effect on charge-transfer ability. It is noteworthy to mention that the $CoPt_{0.02}$ alloy CE has the smallest R_{ct} of 0.68 Ω cm^2, indicating the charge-transfer ability of $CoPt_{0.02}$ is the highest. The conclusions for the electrocatalytic activity and diffusion derived from EIS and CV data are consistent.

Figure 6b gives the EIS spectra of dummy cell from $CoPt_{0.02}$ alloy to examine the electrochemical stability of alloy CE. R_{ct} increases from 0.68 to 4.25 Ω cm^2, and to 24.28 Ω cm^2 for $CoPt_{0.02}$ after aging for 10 and 40 days, respectively. This indicates that $CoPt_{0.02}$ alloy CE has a relatively electrochemical stability against aging.

Tafel polarization was carried out and presented in Figure 7 by recording on the symmetrical cells to reveal the interfacial

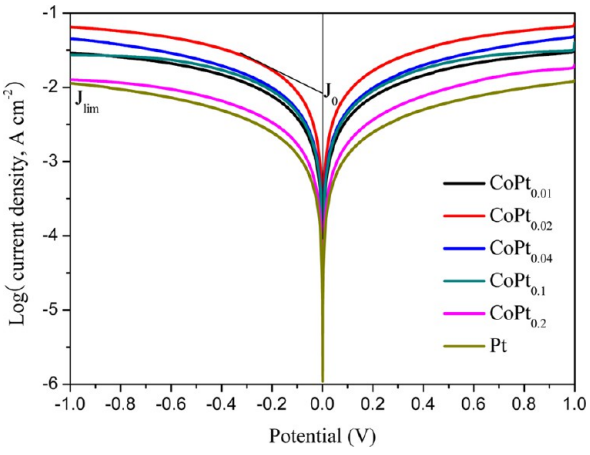

Figure 7. Tafel polarization curves of symmetrical cells fabricated with Pt and CoPt alloy CEs that are same as the ones used in EIS experiments.

charge-transfer properties at the CE/electrolyte interface. The larger slope for the anodic or cathodic branch indicates a higher exchange current density (J_0) on the electrode and better catalytic activity toward triiodide reduction. Apparently, the calculated J_0 also follows an order of $CoPt_{0.02}$ > $CoPt_{0.04}$ > $CoPt_{0.1}$ > $CoPt_{0.01}$ > $CoPt_{0.2}$ > Pt, which match the order of R_{ct}. The elvated J_0 is the result of rapid charge-transfer.[32] The intersection of the cathodic branch with the *Y*-axis can be considered as the limiting diffusion current density (J_{lim}), which determined by the diffusion properties of the redox couple and the CE catalysts. One can see that the J_{lim} also follows an order of $CoPt_{0.02}$ > $CoPt_{0.04}$ > $CoPt_{0.1}$ > $CoPt_{0.01}$ > $CoPt_{0.2}$ > Pt.

CV curves of 100 cycles have been scanned to determine the continuous electrocatalysis of triiodides by $CoPt_{0.02}$ alloy CE as shown in Figure 8. No apparent decrease in peak current density from redox reaction of triiodides is observed, indicating that the CoPt alloy CE can consistently reduce the triiodides into iodides, which is desirable for stable DSSCs.

CONCLUSIONS

In summary, we have demonstrated that electrochemical codeposition of CoPt alloy CEs is an effective strategy for declining the expenses of CE materials and enhancing the photovoltaic performances of DSSCs. $CoPt_{0.02}$ alloy exhibits amazing electrocatalytic activity for the reduction of triiodide ions. The DSSC from $CoPt_{0.02}$ alloy CE provides an impressive power conversion efficiency of 10.23% in comparison with that of 6.52% from pure Pt CE. The research presented here is far from being optimized but these profound advantages along with low-cost synthesis and scalable materials promise the new nanocrystallines to be strong candidates in robust DSSCs.

AUTHOR INFORMATION

Corresponding Author

*E-mail: tangqunwei@ouc.edu.cn. Tel/Fax: 86-532-66781690.

Notes

The authors declare no competing financial interest.

ACKNOWLEDGMENTS

The authors gratefully acknowledge Ocean University of China for providing Seed Fund to this project, and Fundamental Research Funds for the Central Universities (201313001, 201312005), Shandong Province Outstanding Youth Scientist Foundation Plan (BS2013CL015), Doctoral Fund of Ministry of Education of China (20130132120023), Shandong Provincial Natural Science Foundation (ZR2011BQ017), and Research Project for the Application Foundation in Qingdao (13-1-4-198-jch).

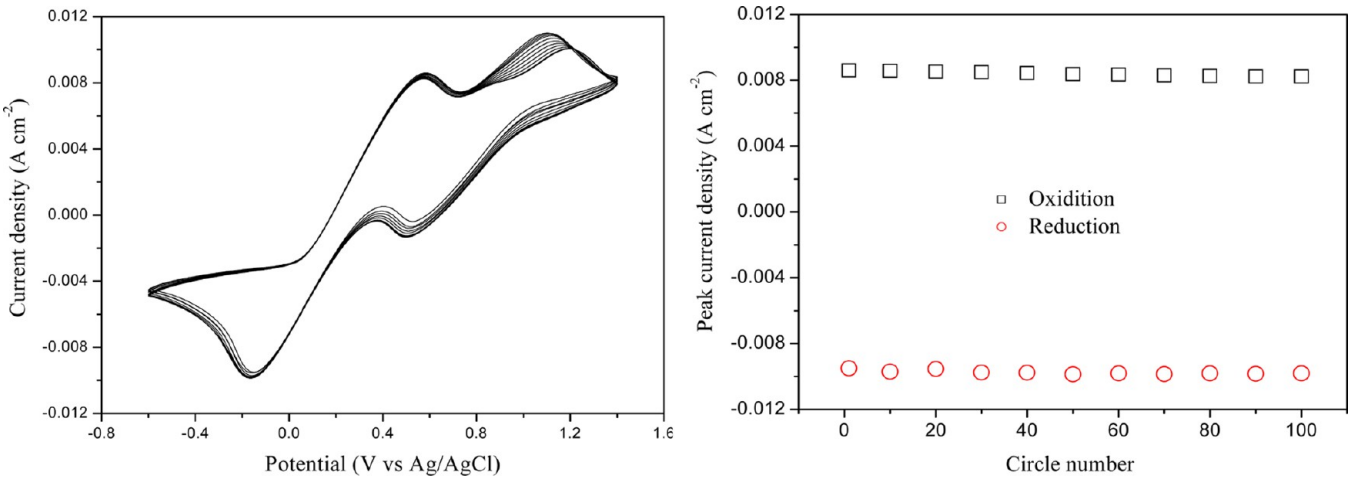

Figure 8. (a) CV curves of 100 cycles using $CoPt_{0.02}$ as working electrode at a scan rate of 50 mV s^{-1}. (b) The peak current density stability as a function of cycle.

REFERENCES

(1) O'Regan, B.; Grätzel, M. A Low-Cost, High-Efficiency Ssolar Cell Based on Dye-Sensitized Colloidal TiO_2 Films. *Nature* **1991**, *353*, 737−740.

(2) Ye, Y.; Jo, C.; Jeong, I.; Lee, J. Functional Mesoporous Materials for Energy Applications: Solar Cells, Fuel Cells, and Batteries. *Nanoscale* **2013**, *5*, 4584−4605.

(3) Poudel, P.; Qiao, Q. One Dimensional Nanostructure/Nanoparticle Composites as Photoanodes for Dye-Sensitized Solar Cells. *Nanoscale* **2012**, *4*, 2826−2838.

(4) Ito, S.; Zakeeruddin, S. M.; Comte, P.; Liska, P.; Kuang, D.; Grätzel, M. Bifacial Dye-Sensitized Solar Cells Based on an Ionic Liquid Electrolyte. *Nat. Photonics* **2008**, *2*, 693−698.

(5) Li, G. R.; Wang, F.; Jiang, Q. W.; Gao, X. P.; Shen, P. W. Carbon Nanotubes with Titanium Nitride as a Low-Cost Counter-Electrode Material for Dye-Sensitized Solar Cells. *Angew. Chem., Int. Ed.* **2010**, *49*, 3653−3656.

(6) Wang, H.; Sun, K.; Tao, F.; Stacchiola, D. J.; Hu, Y. H. Honey-Nest-Like Structured Graphene and Its High Efficiency as Counter Electrode Catalysts for Dye-Sensitized Solar Cells. *Angew. Chem., Int. Ed.* **2013**, *52*, 9210−9214.

(7) Tang, Q. W.; Cai, H. Y.; Yuan, S. S.; Wang, X. Counter Electrodes from Double-Layered Polyaniline Nanostructures for Dye-Sensitized Solar Cell Applications. *J. Mater. Chem. A* **2013**, *1*, 317−323.

(8) Li, Q. H.; Wu, J. H.; Tang, Q. W.; Lan, Z.; Li, P. J.; Lin, J. M.; Fan, L. Q. Application of Microporous Polyaniline Counter Electrode for Dye-Sensitized Solar Cells. *Electrochem. Commun.* **2008**, *10*, 1299−1302.

(9) Tai, Q.; Chen, B.; Guo, F.; Xu, S.; Hu, H.; Sebo, B.; Zhao, X. Z. In Situ Prepared Transparent Polyaniline Electrode and Its Application in Bifacial Dye-Sensitized Solar Cells. *ACS Nano* **2011**, *5*, 3795−3799.

(10) Han, J.; Kim, H.; Kim, D. Y.; Jo, S. M.; Jang, S. Y. Water-Soluble Polyelectrolyte-Grafted Multiwalled Carbon Nanotube Thin Films for Efficient Counter Electrode of Dye-Sensitized Solar Cells. *ACS Nano* **2010**, *4*, 3503−3509.

(11) Gong, F.; Wang, H.; Xu, X.; Zhou, G.; Wang, Z. S. In Situ Growth of $Co_{0.85}Se$ and $Ni_{0.85}Se$ on Conductive Substrates as High-Performance Counter Electrodes for Dye-Sensitized Solar Cells. *J. Am. Chem. Soc.* **2012**, *134*, 10953−10958.

(12) Cheng, X. Y.; Zhou, Z. J.; Hou, Z. L.; Zhou, W. H.; Wu, S. X. High Performance Dye-Sensitized Solar Cell Using $CuInGaSe_2$ as Counter Electrode Prepared by Sputtering. *Sci. Adv. Mater.* **2013**, *5*, 1193−1198.

(13) Xu, Q.; Liu, F.; Liu, Y.; Cui, K.; Feng, X.; Zhang, W.; Huang, Y. Broadband Light Absorption Enhancement in Dye-Sensitized Solar Cells with Au-Ag Alloy Popcorn Nanoparticles. *Sci. Rep.* **2013**, *3*, 2112 (7 pages).

(14) Long, N. V.; Yang, Y.; Thi, C. M.; Minh, N. V.; Cao, Y.; Nogami, M. The Development of Mixture, Alloy, and Core-Shell Nanocatalysts with Nanomaterial Supports for Energy Conversion in Low-Temperature Fuel Cells. *Nano Energy* **2013**, *2*, 636−676.

(15) Zheng, F.; Alayoglu, S.; Pushkarev, V. V.; Beaumont, S. K.; Specht, C.; Aksoy, F.; Liu, Z.; Guo, J.; Somorjai, G. A. In Situ Study of Oxidation States and Structure of 4 nm CoPt Bimetallic Nanoparticles During CO Oxidation Using X-ray Spectroscopies in Comparison with Reaction Turnover Frequency. *Catal. Today* **2012**, *182*, 54−59.

(16) Ahn, S. H.; Kwon, O. J.; Kim, S. K.; Choi, I.; Kim, J. J. Electrochemical Preparation of Pt-Based Ternary Alloy Catalyst for Direct Methanol Fuel Cell Anode. *Int. J. Hydrogen Energy* **2010**, *35*, 13309−13316.

(17) Zeng, W.; Fang, G.; Wang, X.; Zheng, Q.; Li, B.; Huang, H.; Tao, H.; Liu, N.; Xie, W.; Zhao, X.; Zou, D. Hierarchical Porous Nano-Carbon Composite: Effective Fabrication and Application in Dye Sensitized Solar Cells. *J. Power Sources* **2013**, *229*, 102−111.

(18) Park, S. H.; Kim, B. K.; Lee, W. J. Electrospun Activated Carbon Nanofibers with Hollow Core/Highly Mesoporous Shell Structure as Counter Electrodes for Dye-Sensitized Solar Cells. *J. Power Sources* **2013**, *239*, 122−127.

(19) Yousef, A.; Akhtar, M. S.; Barakat, N. A. M.; Motlak, M.; Yang, O. B.; Kim, H. Y. Effective NiCu NPs-Doped Carbon Nanofibers as Counter Electrodes for Dye-Sensitized Solar Cells. *Electrochim. Acta* **2013**, *102*, 142−148.

(20) Shin, S. S.; Kim, J. S.; Suk, J. H.; Lee, K. D.; Kim, D. W.; Park, J. H.; Cho, I. S.; Hong, K. S.; Kim, J. Y. Improved Quantum Efficiency of Highly Efficient Perovskite $BaSnO_3$-Based Dye-Sensitized Solar Cells. *ACS Nano* **2013**, *7*, 1027−1035.

(21) Wang, M. K.; Anghel, A. M.; Marsan, B.; Ha, N. C.; Pootrakulchote, N.; Zakeeruddin, S. M.; Grätzel, M. CoS Supersedes Pt as Efficient Electrocatalyst for Triiodide Reduction in Dye-Sensitized Solar Cells. *J. Am. Chem. Soc.* **2009**, *131*, 15976−15977.

(22) Huang, Z.; Liu, X. Z.; Li, K. X.; Li, D. M.; Luo, Y. H.; Li, H.; Song, W. B.; Chen, L. Q.; Meng, Q. B. Application of Carbon Materials as Counter Electrodes of Dye-Sensitized Solar Cells. *Electrochem. Commun.* **2007**, *9*, 596−598.

(23) Shao, Y.; Liu, J.; Wang, Y.; Lin, Y. Novel Catalyst Support Materials for PEM Fuel Cells: Current Status and Future Prospects. *J. Mater. Chem.* **2009**, *19*, 46−59.

(24) Morozan, A.; Jousselme, B.; Palacin, S. Low-Platinum and Platinum-Free Catalysts for the Oxygen Reduction Reaction at Fuel Cell Cathodes. *Energy Environ. Sci.* **2011**, *4*, 1238−1254.

(25) Yu, P.; Pemberton, M.; Plasse, P. PtCo/C Cathode Catalyst for Improved Durability in PEMFCs. *J. Power Sources* **2005**, *144*, 11−20.

(26) Nam, K. W.; Song, J.; Oh, K. H.; Choo, M. J.; Park, H.; Park, J. K.; Choi, J. W. Monodispersed PtCo Nanoparticles on Hexadecyltrimethylammonium Bromide Treated Graphene as an Effective Oxygen Reduction Reaction Catalyst for Proton Exchange Membrane Fuel Cells. *Carbon* **2012**, *50*, 3739−3747.

(27) Xu, C.; Hou, J.; Pang, X.; Li, X.; Zhu, M.; Tang, B. Nanoporous PtCo and PtNi Alloy Ribbons for Methanol Electrooxidation. *Int. J. Hydrogen Energy* **2012**, *37*, 10489−10498.

(28) Wang, G. J.; Gao, Y. Z.; Wang, Z. B.; Du, C. Y.; Wang, J. J.; Yin, G. P. Investigation of PtNi/C Anode Electrocatalysts for Direct Borohydride Fuel Cell. *J. Power Sources* **2010**, *195*, 185−189.

(29) Tributsch, H. Dye Sensitization Solar Cells: A Critical Assessment of the Learning Curve. *Coordin. Chem. Rev.* **2004**, *248*, 1511−1530.

(30) Daeneke, T.; Mozer, A. J.; Kwon, T. H.; Duffy, N. W.; Holmes, A. B.; Bach, U.; Spiccia, L. Dye Regeneration and Charge Recombination in Dye-Sensitized Solar Cells with Ferrocene Derivatives as Redox Mediators. *Energy Environ. Sci.* **2012**, *5*, 7090−7099.

(31) Lv, Z. B.; Yu, J. F.; Wu, H. W.; Shang, J.; Wang, D.; Hou, S. C.; Fu, Y. P.; Wu, K.; Zou, D. C. Highly Efficient and Completely Flexible Fiber-Shaped Dye-Sensitized Solar Cell Based on TiO_2 Nanotube Array. *Nanoscale* **2012**, *4*, 1248−1253.

(32) Li, Q. H.; Chen, X. X.; Tang, Q. W.; Xu, H. T.; He, B. L.; Qin, Y. C. Imbibition of Polypyrrole Into Three-Dimensional Poly-(Hydroxyethyl Methacrylate/Glycerol) Gel Electrolyte for Robust Quasi-Solid-State Dye-Sensitized Solar Cells. *J. Mater. Chem. A* **2013**, *1*, 8055−8060.